Numerical Investigation of the Shock Interaction Effect on the Lateral Jet Controlled Missile

Byung-Young Min, Jae-Woo Lee, and Yung-Hwan Byun
Dept. of Aerospace Engineering, Konkuk University
1 Hwayang, Gwangjin, Seoul, 143-701 Korea
jwlee@konkuk.ac.kr

Keywords: Lateral Jet, Shock Interaction

Abstract

A computational study on the supersonic flow around the lateral jet controlled missile has been performed. Case studies have been performed by comparing the normal force coefficient and the moment coefficient of a missile body for several different jet flow conditions, angle of attacks, circumferential jet locations, and spouting jet angles. For the several different jet flow conditions, which include the jet pressure, the jet Mach number, and the corresponding jet mass flow rate, the results show that the normal force coefficient is almost proportional to the jet thrust but the moment coefficient is not. Distinctly different flow phenomena can be noticed as the pressure ratio and the jet Mach number increase. By investigating the angle of attack effect to the normal force and the pitching moment, it has been identified that the normal force and the pitching moment show nonlinearity with respect to the angle of attack. From the detailed flow field analyses with respect to the jet flow conditions and the angle of attacks, it is verified that most of the normal force loss and the pitching moment generation are taken place at the low-pressure region behind the jet nozzle. Furthermore, the normal force and the pitching moment characteristics of the missile have been identified by comparing different circumferential jet locations and spouting jet angles.

Nomenclature

C_M : moment coefficient ($C_M = M/qSd$)
C_N : normal force coefficient($C_N = N/qS$)
C_T : jet thrust ratio ($C_T = T_{jet}/qS$)
C_P : pressure coefficient
d : missile diameter [m]
M : moment [N·m]
M_{jet} : jet Mach number
$\dot{m}_{jet}$: mass flow rate of jet [kg/s]
N : normal force [N]
P_{ratio} : jet pressure ratio ($P_{ratio} = P_{jet}/P_{\infty}$)
q : dynamic pressure
S : missile cross-sectional area [m^2]
T_{jet} : jet thrust [N]
α : angle of attack
θ : circumferential angle around the missile body
ψ : spouting jet angle

Subscripts

FU : forebody upper-side of missile
FL : forebody lower-side of missile
jet : with-jet condition
jetoff : no-jet condition
RU : rear body upper-side of missile
RL : rear body lower-side of missile
∞ : freestream condition

Introduction

Existing fin controlled missiles have delayed response time and limitations on maneuvering at low velocity or high altitude because they are controlled by the moments produced at the control surfaces that need high dynamic pressure. On the other hand, the lateral jet controlled missiles have short response time and high maneuverability even at low velocity and low-density area. Therefore, the lateral jet attitude control has been a preferred concept as a new missile defense system[1].

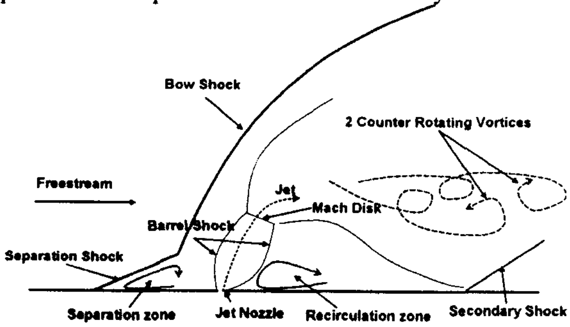

Fig. 1 Complicated flow structure around jet nozzle[2]

As shown at Fig. 1, the aerodynamic characteristics of a lateral jet are complicated because of the local shock-shock interaction, which consists of separation shock, bow shock, barrel shock and Mach disk around jet nozzle, and the downstream interaction by the counter rotating vortices[2]. By the separation shock and bow shock interaction, a high-pressure region is formed in front of the lateral jet nozzle, and a low-pressure region is generated behind the jet nozzle because of the suction effect by lateral jet. Therefore, a pitch down moment is generated at the jet nozzle, which locates at the center of gravity of the missile. Moreover, when the lateral jet is applied to the three-dimensional bodies such as missiles, the bow shock in front of the jet nozzle wraps around the body and generates a high-pressure region at the opposite side of jet nozzle, which reduces the lateral jet performance[3]. These phenomena are affected by the jet nozzle arrangement, the jet configuration parameters and the jet flow characteristics such as jet spouting angle, jet thrust, jet nozzle location, and jet nozzle shape[1,3,4]. Therefore, for the effective lateral jet controlled missile design, the influence of those parameters must be studied thoroughly.

In this study, as a preliminary study of the optimum design of the lateral jet guided missile, the paper will investigate the effect of several jet flow conditions, angle of attack, circumferential jet nozzle location and spouting jet angle by comparing the normal force coefficient and the moment coefficient.

There are two kinds of missile attitude control types using lateral jet. First, by locating the jet at the center of gravity point of the missile, a transition movement of missile can be obtained without any pitching moment generation. The other type is to control the missile attitude using the pitching moment generated by the jet located at a certain distance from the missile center of gravity. In this study, the first type, a lateral jet located at the center of gravity, is considered. Therefore, the generation of the pitching moment is negative effect to the missile control and should be diminished.

Aerodynamic Analysis Method

For the analysis of complex flow phenomena around the lateral jet controlled missile, a three-dimensional Navier-Stokes computer code, AADL3D, is developed for the unsteady, compressible flow. Spalart-Allmaras one equation turbulence model is implemented for relatively rapid computational time[5].

Roe's FDS(flux difference splitting) scheme is implemented for the spatial discretization with the MUSCL for higher order extension. The minmod limiter is used to remove solution oscillations. Central difference scheme is used for the calculation of viscous flux term and fully implicit LU-SGS scheme is employed for time integration. The developed analysis code has been validated through several supersonic examples which have experimental data: the ogive-cylinder with angles of attack, freestream-jet interaction on the flat plate and simple missile body with lateral jet with angles of attack[6].

Case Studies of Lateral Jet Controlled Missile

Grid System Selection

The missile configuration for the case studies is simple tangent ogive-cylinder body without fin, as shown at Fig. 3. To increase the computational efficiency, a grid system, which is coarse but can guarantee solution accuracy, is selected by investigating the convergence rate and the converged solutions of several grid systems.

The freestream Mach number was 2.6 and jet Mach number was 2.04. P_{ratio} was 45.7 and the Reynolds number was 6.63×10^6. Atmospheric condition of 10km altitude was used. From the results of Fig. 2, the 95×34×33 grid system has been selected, and the grid system is shown at Fig. 3.

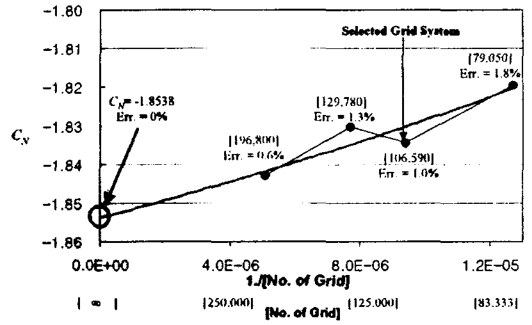

Fig. 2 Result of grid density test

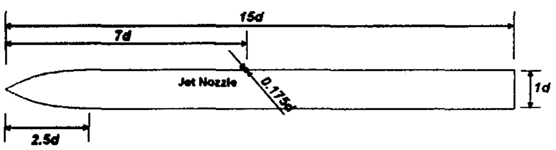

(a) Missile configuration for the case studies

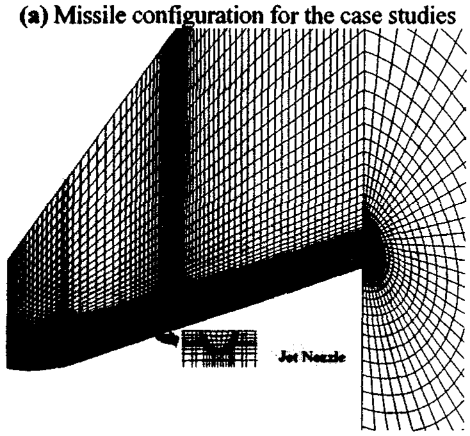

(b) Selected grid system (95×34×33)

Fig. 3 Missile configuration and grid system

Free-stream and Analysis Conditions

For the different pressure ratios and the jet Mach number variations, the normal force and the moment coefficients of a missile body are compared to find out the effect of the jet flow characteristics on the missile attitude control. For all calculations for the different jet flow condition effect, the freestream Mach number is 2.6 and the Reynolds number is 6.63×10^6. Table 1 summarizes the jet flow conditions of each case.

The missile configuration is nondimensionalized by the missile diameter, *d*, and is represented at Fig. 3. Force, moment and other nomenclatures are defined at Fig. 4.

Case 1, 2 and 3 are selected to compare the jet pressure effect while fixing the jet Mach number, and Case 1, 4 and 5 are compared to find the jet Mach number effect while fixing the jet pressure ratio. Case 2 and 4 have the same mass flow rate increment as Case 1.

Table 1 Jet flow conditions for each case

	Case 1	Case 2	Case 3	Case 4	Case 5	Case 6
P_{ratio}	150	300	450	150	150	850
M_{jet}	1	1	1	2	3	1
$\dot{m}_{jet}$ [kg/s]	14.04	28.08	42.12	28.08	42.12	79.56
C_T	2.32	4.65	6.98	6.40	13.20	13.20

Case 3 and 5 also have the same mass flow rate increment as Case 1. Case 5 and 6 have the same jet thrust.

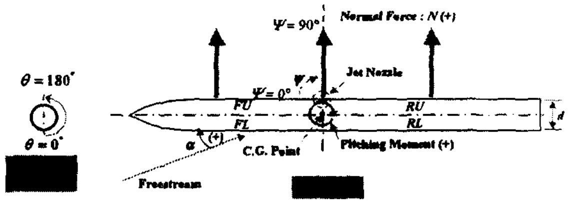

Fig. 4 Nomenclature definition

Furthermore, to find out the effect of the angle of attack, circumferential jet location and the spouting jet angle on the normal force and the pitching moment characteristics of the missile, analyses are performed for five different angle of attack (α=-20°, -10°, 0°, 10°, 20°), five different circumferential jet locations (θ=0°, 45°, 90°, 135°, 180°) and seven different spouting jet angles (ψ=30°, 45°, 60°, 75°, 90°, 105°, 120°). The analysis condition of freestream and jet of these cases is same as grid system selection case. For the different circumferential jet location case, the angle of attack is set to 10°.

Jet Pressure Variation: Case 1, 2 and 3

Table 2 summarizes the result of the calculations for each case and Fig. 5 shows the pressure contour at the surface of Case 1, 2 and 3. As can be seen at Fig. 5, high and low pressure regions are extended, as the pressure ratio increases. As a result, the moment is increased.

Also, Table 2 shows that the normal force and the pitching moment are almost proportional to the pressure ratio. The normal force is always less than the jet thrust because of the low-pressure region behind the nozzle and high-pressure region caused by wraparound effect of separation shock. The high-pressure region in front of nozzle and the low-pressure region behind nozzle produce most of the pitching moment. Especially, the low-pressure region behind the nozzle contributes to the moment generation greatly.

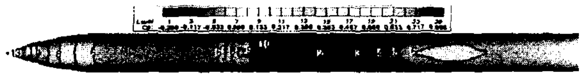

(a) Case 1 (P_{ratio} = 150)

(b) Case 2 (P_{ratio} = 300)

(c) Case 3 (P_{ratio} = 450)

Fig. 5 C_p contour on the surface

Jet Mach Number Variation: Case 1, 4 and 5

Fig. 6 and 7 show the pressure contour on the surface and Mach contour on the symmetry plane of Case 1, 4 and 5. As the jet Mach number increases, the inclination and the size of the barrel shock become steeper and larger while the thickness near the surface becomes thinner (Fig. 7). Therefore, the high-pressure region in front of the jet nozzle decreases as the jet Mach number increases (Fig. 6). Moreover, the low-pressure region right behind the nozzle decreases as the jet Mach number increases. Figure 8 helps to understand the phenomena. The inclination of the barrel shock becomes steeper as the jet Mach number increases, therefore, suction effect by the jet is reduced, and the propagated vortices are apart from the surface, hence, the effect of vortices to the surface is reduced.

Table 2 shows that the normal force and the pitching moment are proportional to the jet thrust. However, Case

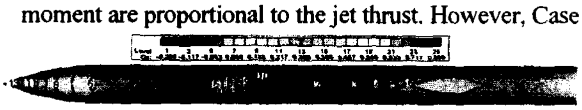

(a) Case 1(M_{jet} = 1)

(b) Case 4(M_{jet} = 2)

(c) Case 5(M_{jet} = 3)

Fig. 6 C_p contour on the surface

Table 2 The results of calculations for different jet flow condition effect

	P_{ratio}	M_{jet}	C_T	C_N	$C_{N_{FU}}$	$C_{N_{FL}}$	$C_{N_{RU}}$	$C_{N_{RL}}$	C_M	$C_{M_{FU}}$	$C_{M_{FL}}$	$C_{M_{RU}}$	$C_{M_{RL}}$
Case 1	150	1	2.323	**-2.067**	-0.236	0.099	**0.426**	-0.034	**-0.302**	-0.162	0.053	**-0.701**	0.508
Case 2	300	1	4.653	**-4.254**	-0.376	0.144	**0.689**	-0.058	**-0.825**	-0.224	0.084	**-1.511**	0.827
Case 3	450	1	6.983	**-6.440**	-0.470	0.205	**0.903**	-0.095	**-1.660**	-0.330	0.156	**-2.533**	1.046
Case 4	150	2	6.401	**-6.028**	-0.373	0.118	**0.661**	-0.032	**-0.981**	-0.187	0.059	**-1.686**	0.833
Case 5	150	3	13.196	**12.837**	-0.436	0.122	**0.641**	0.032	**-1.613**	-0.197	0.059	**-2.077**	0.602

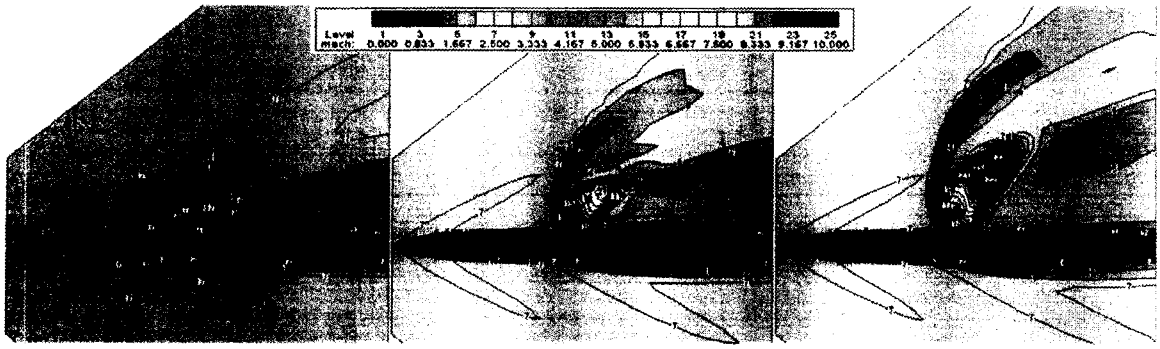

(a) Case 1($M_{jet} = 1$)　　(b) Case 4($M_{jet} = 2$)　　(c) Case 5($M_{jet} = 3$)

Fig. 7 Mach number contour

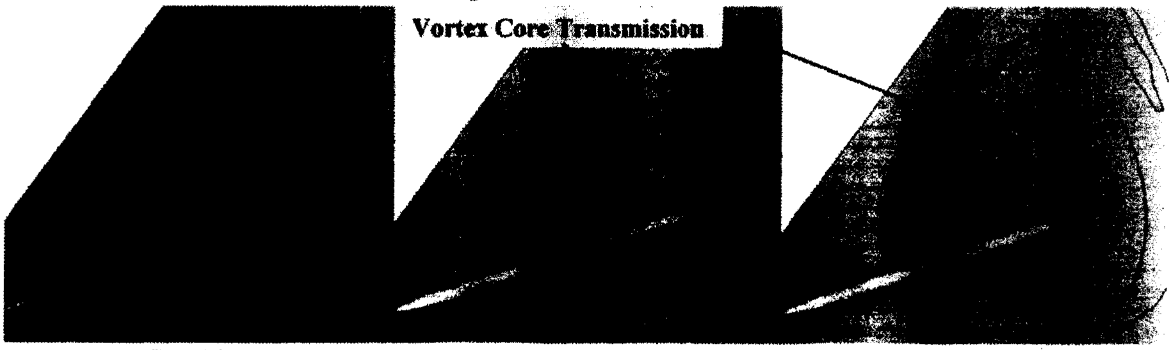

(a) Case 1($M_{jet} = 1$)　　(b) Case 4($M_{jet} = 2$)　　(c) Case 5($M_{jet} = 3$)

Fig. 8 Mach number contour and the path of the vortex

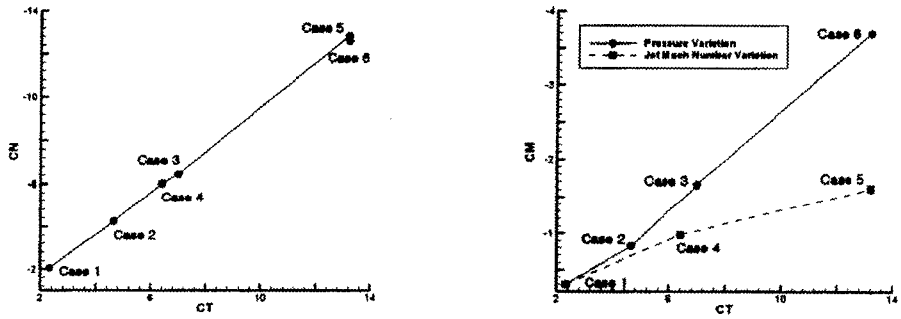

(a) C_N vs. C_T　　(b) C_M vs. C_T

Fig. 9 C_N, C_M vs. C_T plots

5 generates less pitch down moment than Case 3 with same mass flow rate and higher jet thrust.

Figure 9 shows the relationship of the normal force and the moment coefficients according to the thrust ratio. The normal force is almost proportional to the jet thrust but the moment does not have the same tendency. The case study shows that the moment is not only a function of the jet thrust but also the jet pressure and Mach number. The increased jet thrust by increasing jet Mach number produces smaller pitch down moment than the same thrust with increased jet pressure because the effect of vortices on the surface is reduced as the jet Mach number increases.

Angle of Attack Effect

Figure 10 shows Mach number contour and the vortex core transmission, generated from the freestream-jet interaction for the angle of attack of -20°, 0° and 20°. At $\alpha = 20°$, the upper side vortex generated by the jet is far apart from the surface. As a result, the influence of the vortex on the missile surface is relatively small. In contrast, at $\alpha = -20°$, the generated vortex is bent by the freestream, and it sweeps the missile surface, as a result, vortex prevents the downward freestream hits the missile surface. Therefore, strong bow shock effect caused by downward freestream velocity component is vanished above upper rear body surface, and more large low-pressure region is formed compared to jet-off case.

Figure 11 and 12 show pressure contour at the symmetry plane and the missile surface. At the negative angle of attack (the windward jet), there is a strong bow shock in front of the jet nozzle, which contributes to increase the normal force. Although the pressure rises at upper rear body surface because of the presence of the secondary shock at the upper rear

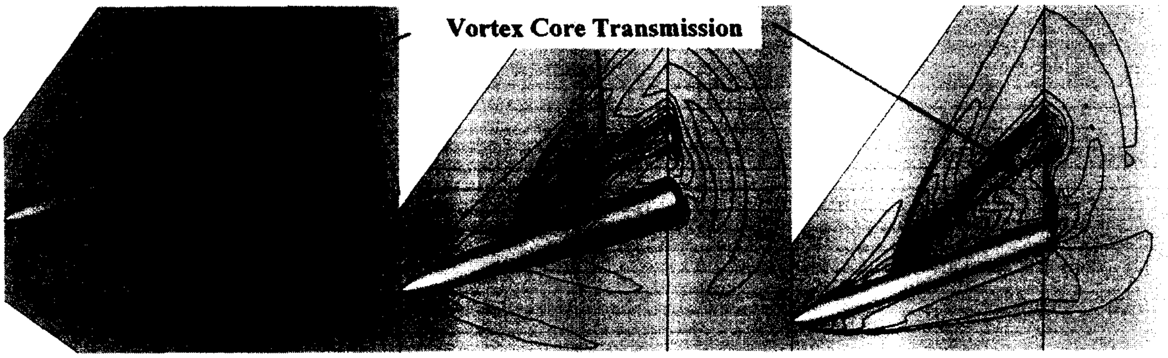

(a) α = -20° (b) α = 0° (c) α = 20°

Fig. 10 Mach number contour and vortex core transmission

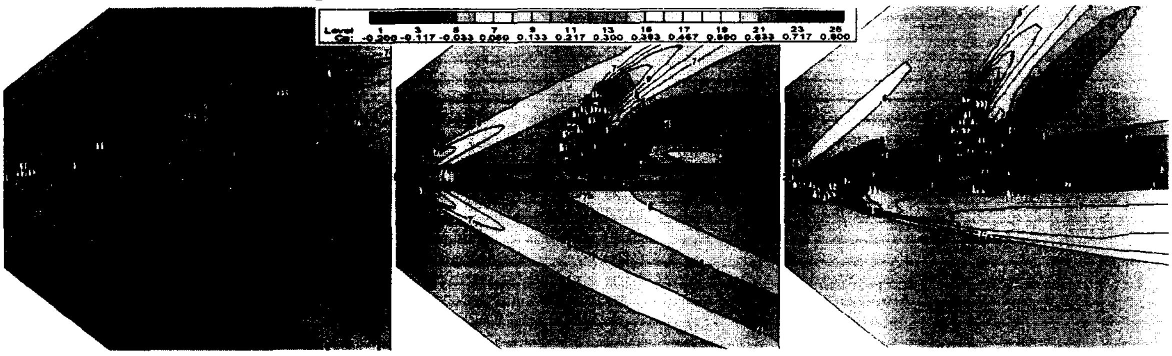

(a) α = -20° (b) α = 0° (c) α = 20°

Fig. 11 C_p contour at the symmetry plane

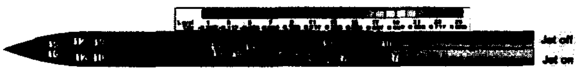

(a) α = -20°

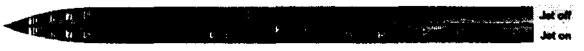

(b) α = 0°

(c) α = 20°

Fig. 12 C_p contour on the surface

body surface at α = -20°, lower pressure distribution is obtained near the region behind the jet than that of the jet off case. Therefore the jet results in a greater normal force loss and pitch down moment because of the freestream-jet interaction. In contrast, at α = 20°, there is very little difference in pressure distribution between jet off case and the jet-on case. Table 3 and Fig. 13 compare the normal force and the pitching moment coefficients caused by jet effect for different angles of attack.

As shown at Table 3 and Fig. 13, a negative angle of attack (windward jet) causes a relatively big normal force loss and pitch down moment compared with the positive angle of attack case (leeward jet). The main reason is the formation of the low-pressure region behind the nozzle. Furthermore, the behaviors of the normal force and the pitch down moment by the jet for different angle of attack show high nonlinearity especially near the high negative angle of attack.

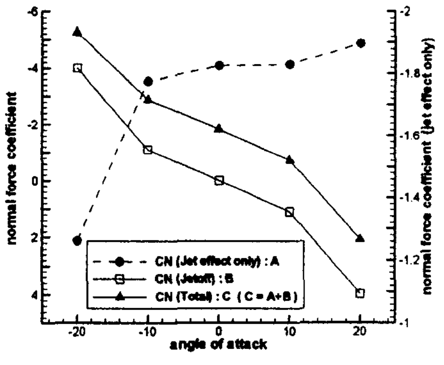

(a) C_N *vs.* angle of attack

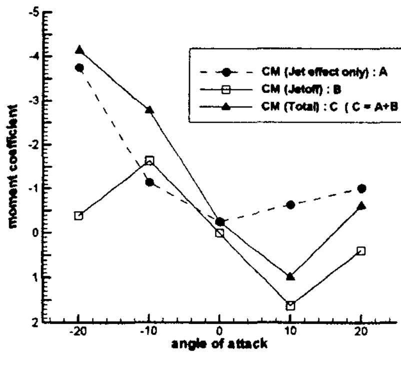

(b) C_M *vs.* angle of attack

Fig. 13 C_N, C_M *vs.* angle of attack plots

Table 3 The comparison of calculated results for angle of attack effect (jet effect only)

α	C_N	$C_{N_{FU}}$	$C_{N_{FL}}$	$C_{N_{RU}}$	$C_{N_{RL}}$	C_M	$C_{M_{FU}}$	$C_{M_{FL}}$	$C_{M_{RU}}$	$C_{M_{RL}}$
20°	**-1.896**	-0.203	0.007	**0.284**	0.032	**-1.011**	-0.102	0.002	**-0.836**	-0.075
10°	**-1.829**	-0.167	0.035	**0.256**	0.064	**-0.636**	-0.124	0.013	**-0.591**	0.066
0°	**-1.825**	-0.171	0.041	**0.321**	0.	**-0.255**	-0.079	0.017	**-0.543**	0.351
-10°	**-1.775**	-0.227	0.027	**0.448**	-0.006	**-1.140**	-0.060	0.010	**-1.080**	-0.010
-20°	**-1.262**	-0.287	0.018	**0.944**	0.080	**-3.745**	-0.073	0.006	**-3.148**	-0.529

Circumferential Jet Location Effect

To figure out the effect of the jet location on the aerodynamic characteristics of the missile with angle of attack, analyses have been performed for several circumferential jet locations(θ=0°, 45°, 90°, 135°, 180°) with angle of attack of 10°.

Fig. 14 shows pressure contour on the surface. Table 4 summarizes the results of calculations and represents the normal force and the pitching moment coefficient for each jet location. As shown at Fig. 15, greater normal force loss and pitching down moment were generated when jet nozzle is located at θ=0° than θ=180°. However, maximum normal force and minimum pitching down moment were generated when jet nozzle is located at θ=90° because of the largest high pressure region on the rear body upper surface behind the nozzle, which contributes to the increase of the normal force and to decrease of the pitching down moment, due to the strong bow shock by freestream (Fig. 14), and another low pressure region at the opposite side of the nozzle due to the bent jet by freestream.

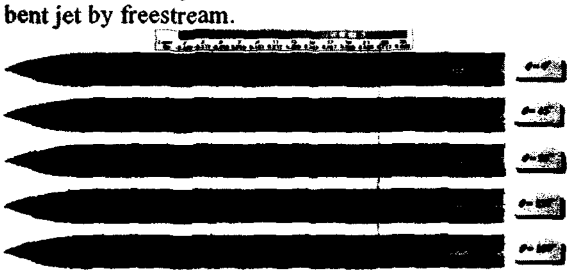

Fig. 14 C_p contour on the surface

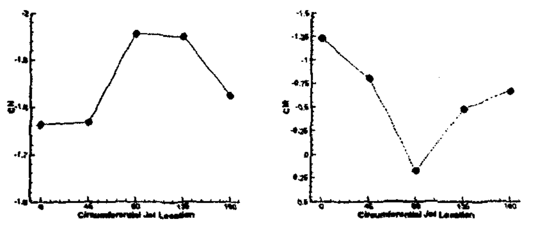

(a) C_N vs. θ (b) C_M vs. θ

Fig. 15 C_N, C_M vs. circumferential jet location plots

Spouting Jet Angle Effect

The attitude control method considered in this study using lateral jet is to obtain a transition movement of missile by locating the jet at the center of gravity point of the missile without any pitching moment generation. But, the previous work shows that the shock interaction effect causes pitching down moment around the jet nozzle, and the main reason of the pitching down moment generation is the low-pressure region on the rear body upper surface, which is formed by the vortex generated by the jet and sweeps over the missile surface. Therefore, as shown at the jet Mach number variation effect, the generated pitching down moment can be decreased by letting the propagating vortex be far apart from the missile surface. Thus, to achieve this effect relatively easily, forward inclination of the spouting jet angle can be considered. Hence, in this study, analyses for several spouting jet angles(ψ= 30°, 45°, 60°, 75°, 90°, 105°, 120°) have been performed and the results were compared.

Fig. 16 and 17 show the pressure contour at the symmetry plane and on the missile surface. Table 5 summarizes the results of calculations and Fig. 18 represents the plotted graph of the results.

As expected, with inclined spouting jet angle in forward direction, the low pressure region behind jet nozzle is decreased and the high pressure region in front of the jet nozzle generated by the bow shock and the separation shock is extended forward. Furthermore, the high-pressure region due to wraparound effect on the opposite side of the jet nozzle moves forward. As a result, as shown in the Fig. 18 and Table 5, pitching down moment is decreased because the low-pressure region behind jet nozzle is decreased which is the major factor for the moment generation as the spouting jet angle is inclined forward. Also, excessively inclined spouting jet angle generates high pressure region by wraparound effect of bow shock and separation shock on the forebody lower side, and it decreases pitching down moment, however, it also decreases normal force, too. However, when the spouting jet angle is inclined forward excessively(below 60° in this study),

Table 4 The comparison of calculated results for jet location effect (jet effect only)

θ	C_N	$C_{N_{FU}}$	$C_{N_{FL}}$	$C_{N_{RU}}$	$C_{N_{RL}}$	C_M	$C_{M_{FU}}$	$C_{M_{FL}}$	$C_{M_{RU}}$	$C_{M_{RL}}$
0°	**-1.763**	-0.23	0.027	**0.465**	-0.008	**-1.231**	-0.063	0.010	**-1.162**	-0.015
45°	**-1.767**	-0.202	0.022	**0.364**	0.036	**-0.8**	-0.058	0.005	**-0.763**	0.017
90°	**-1.956**	-0.169	0.036	**0.193**	0.0	**0.178**	-0.08	0.017	**-0.281**	**0.522**
135°	**-1.950**	-0.177	0.03	**0.174**	0.039	**-0.473**	-0.143	0.015	**-0.503**	0.158
180°	**-1.824**	-0.168	0.036	**0.263**	0.062	**-0.662**	-0.129	0.014	**-0.609**	0.063

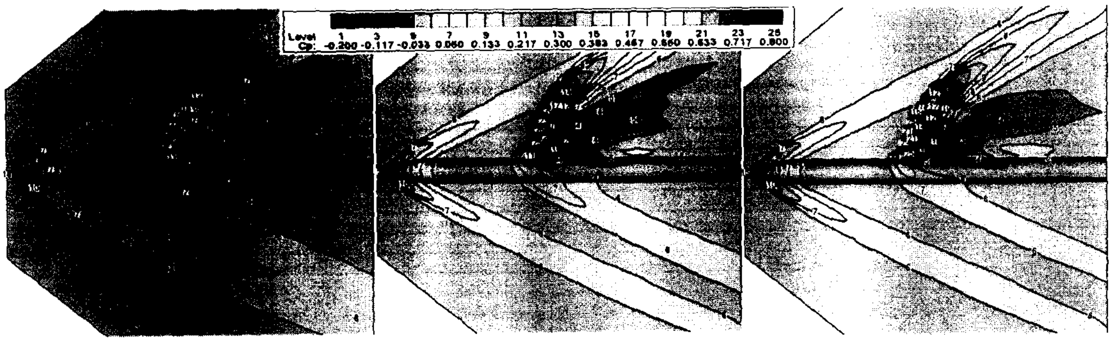

(a) ψ= 45° (b) ψ= 60° (c) ψ= 90°

Fig. 16 C_p contour on the symmetry plane for different spouting jet angle

pitching down moment generation due to the extended high pressure region in front of jet nozzle leads total pitching down moment increase again.

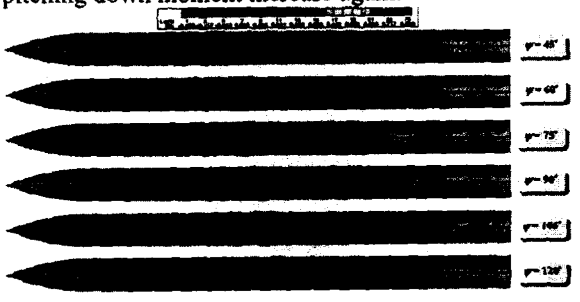

(a) θ=180°

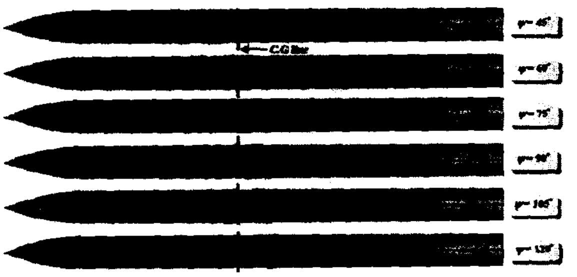

(b) θ=0°

Fig. 17 C_p contour on the surface

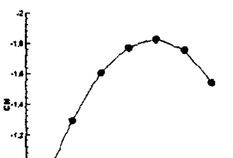

(a) C_N vs. ψ

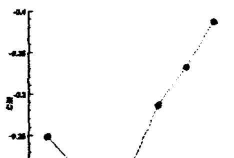

(b) C_M vs. ψ

Fig. 18 C_N, C_M vs. spouting jet angle plots

Normal force becomes maximum when ψ=90° and is decreased as spouting jet angle is inclined forward or backward because the jet thrust is decreased by cosine law.

Conclusion

A computational study of supersonic flow around the lateral jet controlled missile has been performed. To investigate the detailed flowfield, the shock formation, and the surface pressure distribution of the lateral jet controlled missile, several cases with different jet pressure, jet Mach number, jet mass flow rate, angle of attack, circumferential jet location and spouting jet angle were selected and aerodynamic analyses were performed, hence the effect of those factors on the normal force and pitching moment coefficients were analyzed and dominant factors for lateral jet controlled missile have been identified.

The normal force was almost proportional to the jet thrust and there has been thrust loss because of shock interactions. The main reasons of the thrust loss were the formation of the low-pressure region behind the jet nozzle. The pitching moment shows different behavior from the normal force for the several jet pressure and jet Mach number variations. When increasing the jet pressure only, both the high-pressure region in front of jet nozzle and the low-pressure region behind jet nozzle were extended and as a result, the pitching down moment was increased. On the other hand, when increasing jet Mach number only, the high-pressure region was decreased, and the low-pressure region was changed according to the inclination of the barrel shock.

The moment was not only a function of jet thrust, but also of the jet pressure and the jet Mach number. As the jet pressure and the jet Mach number increase, the

Table 5 The results of spouting jet angle effect

ψ	C_T	C_N	$C_{N_{FU}}$	$C_{N_{FL}}$	$C_{N_{RU}}$	$C_{N_{RL}}$	C_M	$C_{M_{FU}}$	$C_{M_{FL}}$	$C_{M_{RU}}$	$C_{M_{RL}}$
30°	**1.008**	**-0.901**	-0.274	**0.230**	**0.256**	-0.104	**-0.249**	**-0.515**	**0.304**	**-0.527**	**0.489**
45°	**1.426**	**-1.291**	-0.270	**0.223**	**0.277**	-0.094	**-0.212**	**-0.461**	**0.262**	**-0.510**	**0.497**
60°	**1.746**	**-1.604**	-0.243	0.092	**0.298**	-0.004	**-0.198**	-0.174	-0.051	**-0.427**	0.352
75°	**1.948**	**-1.771**	-0.210	0.064	**0.322**	0.0	**-0.211**	-0.118	0.029	**-0.490**	0.367
90°	**2.016**	**-1.825**	-0.161	0.042	**0.313**	-0.002	**-0.286**	-0.077	0.014	**-0.554**	0.331
105°	**1.948**	**-1.754**	-0.123	0.024	**0.296**	-0.003	**-0.331**	-0.053	0.011	**-0.556**	0.267
120°	**1.746**	**-1.540**	-0.081	0.010	**0.280**	-0.003	**-0.386**	-0.028	0.003	**-0.561**	0.200

moment increases but when jet Mach number increases and the vortex is apart from the surface then, the pitch down moment increment is reduced because the effect of vortices on the surface are reduced as jet Mach number increases.

The nonlinearity of the normal force and pitch down moment according to the angle of attack has been confirmed. Especially, high negative angle of attack(windward jet) case shows greater normal force loss and the pitch down moment because the bent vortices to the missile body by freestream sweep over rear upper side of the body and enlarge the low-pressure region compared to jet-off case. Therefore, high negative angle of attack maneuver with lateral jet should be avoided.

It is identified that minimum normal force loss and pitching moment were occurred when jet was located at θ=90°.

As spouting jet angle is inclined forward, pitching down moment is decreased because the low-pressure region behind jet nozzle is decreased. However, excessively inclined spouting jet angle to forward causes increase of total pitching moment due to the high-pressure region formed in front of jet nozzle. Thus, a minimum pitching moment can be obtained by selecting proper spouting jet angle in the given condition.

The low-pressure region behind the jet nozzle contributes more greatly to pitch down moment generation than the high-pressure region. Therefore, for the efficient lateral jet attitude control system design, it is identified that the study on reducing the low-pressure region is required.

Further studies will be given to the hot gas or the chemical reaction effect of the spouting jet. In addition, based on the case studies, optimization of lateral jet controlled missile will be performed to find out the most effective flight condition for the missile control.

Acknowledgement

This work was supported by grant number ADD-01-3-1 from the Basic Research Program of the Agency for Defense Development of Korea.

References

1) R. G. Lacau and M. Robert, "The use of Lateral Jet Control at Aerospatiale", Nielsen Engineering & Research, 1988.
2) F. S. Billig, R. C. Orth, and M. Lasky, "A Unified Analysis of Gaseous Jet Penetration", *AIAA Journal*, Vol. 9, No. 6, June 1971, pp.1048-1058.
3) Julius Brandeis and Jacob Gill, "Experimental Investigation of Side-Jet Steering for Supersonic and Hypersonic Missiles", *Journal of Spacecraft and Rockets*, Vol. 33, No. 3, May-June 1996, pp. 346-352.
4) B. Srivastava, "Computational Analysis and Validation for Lateral Jet Controlled Missiles", *Journal of Spacecraft and Rockets*, Vol. 34, No. 5, Sep-Oct 1997, pp. 584-592.
5) Klaus A. Hoffmann and Steve T. Chiang, *Computational Fluid Dynamics, Volume III, Fourth Edition*, Engineering Education System, 2000.
6) Byung-Young Min, *Numerical Analysis and Optimization of Lateral Jet Controlled Missile Using Navier-Stokes Equations*, Master's Thesis, Konkuk University, 2003.